



# Cationic iridacarboranes [3-(arene)-3,1,2-IrC<sub>2</sub>B<sub>9</sub>H<sub>11</sub>]<sup>+</sup> and [3-(MeCN)<sub>3</sub>-3,1,2-IrC<sub>2</sub>B<sub>9</sub>H<sub>11</sub>]<sup>+</sup>: Synthesis, reactivity, and bonding. Catalysis of oxidative coupling of benzoic acid with alkynes



Dmitry A. Loginov, Alena O. Belova, Anna V. Vologzhanina, Alexander R. Kudinov\*

A. N. Nesmeyanov Institute of Organoelement Compounds, Russian Academy of Sciences, 28 ul. Vavilova, 119991 Moscow GSP-1, Russian Federation

## ARTICLE INFO

### Article history:

Received 30 December 2014

Received in revised form

23 January 2015

Accepted 24 January 2015

Available online 19 February 2015

Dedicated to the memory of Academician, Professor Alexander E. Shilov who contributed much to the development of the metal-complex catalyzed C–H activation.

### Keywords:

C–H activation

Iridium

Metal complex catalysis

Metallacarboranes

## ABSTRACT

(Arene)iridacarboranes [3-(arene)-3,1,2-IrC<sub>2</sub>B<sub>9</sub>H<sub>11</sub>]<sup>+</sup> (arene = benzene (**1a**), toluene (**1b**), *o*-xylene (**1c**), *m*-xylene (**1d**), durene (**1e**)) were synthesized by reaction of [(cod)IrCl]<sub>2</sub> with Ti[Ti(η-7,8-C<sub>2</sub>B<sub>9</sub>H<sub>11</sub>)] with the subsequent treatment of the anion [3-(cod)-3,1,2-IrC<sub>2</sub>B<sub>9</sub>H<sub>11</sub>]<sup>-</sup> formed by arenes in refluxing trifluoroacetic acid. Cation **1a** reacts with acetonitrile giving complex [3-(MeCN)<sub>3</sub>-3,1,2-IrC<sub>2</sub>B<sub>9</sub>H<sub>11</sub>]<sup>+</sup> (**2**). Reactions of **2** with Cp<sup>-</sup> anions and arenes afford the cyclopentadienyl and arene derivatives 3-(η-C<sub>5</sub>H<sub>4</sub>R)-3,1,2-IrC<sub>2</sub>B<sub>9</sub>H<sub>11</sub> (R = H (**3a**), C(O)Me (**3b**))) and [3-(arene)-3,1,2-IrC<sub>2</sub>B<sub>9</sub>H<sub>11</sub>]<sup>+</sup> (arene = mesitylene (**1f**), [2,2]paracyclophane (**1g**))). The structures of **1ePF<sub>6</sub>** and **2BF<sub>4</sub>** were determined by X-ray diffraction. According to energy decomposition analysis, the metal–benzene bonding in the iridium cation **1a** is stronger than in the rhodium analog [3-(η-C<sub>6</sub>H<sub>6</sub>)-3,1,2-RhC<sub>2</sub>B<sub>9</sub>H<sub>11</sub>]<sup>+</sup> but weaker than in [(C<sub>5</sub>R<sub>5</sub>)Ir(C<sub>6</sub>H<sub>6</sub>)]<sup>2+</sup>. In the presence of Ag<sub>2</sub>CO<sub>3</sub>, iridacarboranes **1a** and **2** catalyze the oxidative coupling of benzoic acid with diphenylacetylene selectively giving 3,4-diphenylisocoumarin in 40–50% yields. In contrast, the reactions catalyzed by [3,3-Cl<sub>2</sub>-4-SMe<sub>2</sub>-3,1,2-IrC<sub>2</sub>B<sub>9</sub>H<sub>10</sub>]<sub>2</sub> and [CpIr<sub>2</sub>]<sub>2</sub> afford only 1,2,3,4-tetraphenylnaphthalene in 10 and 35% yields, respectively. The iridium catalyzed decarboxylation of benzoic acid was analyzed by DFT calculations.

© 2015 Elsevier B.V. All rights reserved.

## Introduction

Shilov was a pioneer in development of metal-complex catalyzed C–H functionalization of hydrocarbons. In particular, he shown that complexes of Pt(II) and Pt(IV) are capable of functionalizing the C–H bonds of methane [1]. This work started the extensive study of similar systems which was named “Shilov's chemistry” [2].

The cyclopentadienyl complexes [Cp<sup>\*</sup>MCl<sub>2</sub>]<sub>2</sub> (M = Rh, Ir) proved to be effective catalysts for C–H activation [3]. In particular, they catalyze the oxidative coupling of benzoic acids with internal alkynes giving isocoumarin and naphthalene derivatives [4]. The selectivity strongly depends on metal nature. Thus, the rhodium complex [Cp<sup>\*</sup>RhCl<sub>2</sub>]<sub>2</sub> catalyzes this reaction predominantly giving isocoumarins, while the iridium derivative [Cp<sup>\*</sup>IrCl<sub>2</sub>]<sub>2</sub> results in naphthalenes.

Although the dicarboride anion [C<sub>2</sub>B<sub>9</sub>H<sub>11</sub>]<sup>2-</sup> is isolobal with Cp<sup>-</sup> [5], the catalytic activity of metallacarboranes often differs from that of cyclopentadienyl complexes [6]. Therefore, metallacarboranes have found a wide range of applications in catalysis [7]. Recently, we found that rhodacarboranes [3-(η-C<sub>6</sub>H<sub>6</sub>)-3,1,2-RhC<sub>2</sub>B<sub>9</sub>H<sub>11</sub>]<sup>+</sup> and [1,1-I<sub>2</sub>-12-<sup>t</sup>BuNH-1,2,4,12-RhC<sub>3</sub>B<sub>8</sub>H<sub>10</sub>]<sub>2</sub> catalyze oxidative coupling of benzoic acid with diphenylacetylene giving 1,2,3,4-tetraphenylnaphthalene in contrast to [Cp<sup>\*</sup>RhCl<sub>2</sub>]<sub>2</sub> (giving isocoumarins) [8]. Apparently, the difference in selectivity is due to different electronic effects of carborane and Cp ligands.

Herein we report synthesis, reactivity and catalytic activity of cationic iridacarboranes [3-(arene)-3,1,2-IrC<sub>2</sub>B<sub>9</sub>H<sub>11</sub>]<sup>+</sup> and [3-(MeCN)<sub>3</sub>-3,1,2-IrC<sub>2</sub>B<sub>9</sub>H<sub>11</sub>]<sup>+</sup>. The mechanisms of the reactions were studied by DFT computation.

## Results and discussion

### Synthesis

Recently, we have described useful one-pot procedure for the synthesis of (benzene)rhodacarborane [3-(η-C<sub>6</sub>H<sub>6</sub>)-3,1,2-

\* Corresponding author.

E-mail address: [arkudinov@ineos.ac.ru](mailto:arkudinov@ineos.ac.ru) (A.R. Kudinov).

$\text{RhC}_2\text{B}_9\text{H}_{11}^+$  starting from easily available  $[(\text{cod})\text{RhCl}]_2$  and thallium dicarbollide [9]. In present work we used a similar approach for the synthesis of (arene)iridacarboranes [3-(arene)-3,1,2-IrC<sub>2</sub>B<sub>9</sub>H<sub>11</sub>]<sup>+</sup> (arene = benzene, toluene, o- and m-xylene, durene) (**1a–e**) (Scheme 1). Reaction of  $[(\text{cod})\text{IrCl}]_2$  with  $\text{Ti}[\text{Ti}(\eta\text{-7,8-C}_2\text{B}_9\text{H}_{11})]$  preliminarily gives anion  $[3\text{-}(\text{cod})\text{-}3,1,2\text{-IrC}_2\text{B}_9\text{H}_{11}]^-$  (not isolated in pure form). Refluxing of the latter in the presence of arenes in trifluoroacetic acid affords (arene)iridacarboranes **1a–e** in moderate yields (20–40%).

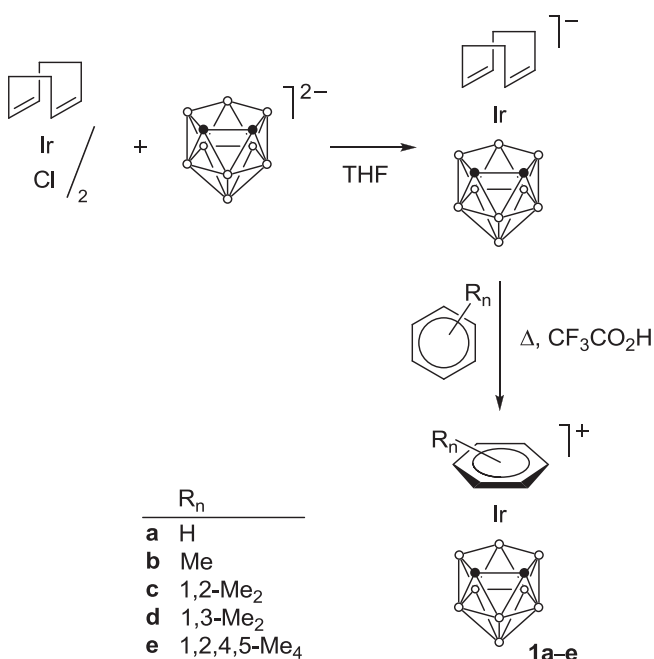
In the <sup>1</sup>H NMR spectra of **1a–e** the signals for the arene ring protons undergo downfield shift with respect to the free arene in contrast to other monocationic arene complexes with carbocyclic ligands in which these signals are usually upfield shifted. Probably, the electron-withdrawing effect of carborane ligand overrides the opposite effect of coordination to the transition metal atom [10]. Similar pattern was observed earlier for the dicationic complexes  $[\text{Cp}^*\text{Ir}(\text{arene})]^2+$  and  $[3\text{-}(\text{arene})\text{-}4\text{-SMe}_2\text{-}3,1,2\text{-IrC}_2\text{B}_9\text{H}_{11}]^2+$  [11,12].

Earlier, we found that the rhodium benzene complex  $[3\text{-}(\eta\text{-C}_6\text{H}_6)\text{-}3,1,2\text{-RhC}_2\text{B}_9\text{H}_{11}]^+$  is substitutionally labile and easily undergoes the arene exchange reaction [9]. The iridium analog **1a** proved to be less reactive. In particular, after refluxing of **1a** with anisole in nitromethane during 6 h the degree of conversion for arene exchange was ca. 14%, according to <sup>1</sup>H NMR. Nevertheless, we found that the refluxing of **1a** in acetonitrile results in quantitative elimination of benzene giving the tris(acetonitrile) derivative  $[3\text{-}(\text{MeCN})_3\text{-}3,1,2\text{-IrC}_2\text{B}_9\text{H}_{11}]^+$  (**2**) in high yield (89%) (Scheme 2).

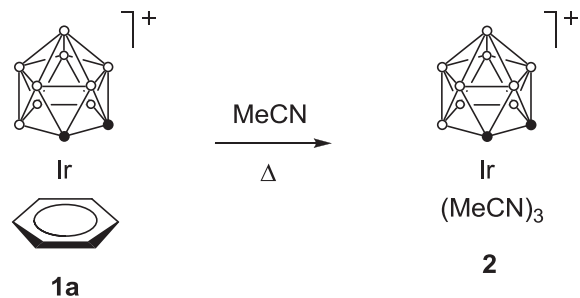
The  $\text{PF}_6^-$  and  $\text{BF}_4^-$  salts of acetonitrile cation **2** are stable in air for long time. Nevertheless, the acetonitrile ligands in **2** are much more labile than the benzene ligand in **1a**. Therefore complex **2** can be used as a useful synthon of the cationic iridacarborane fragment  $[3,1,2\text{-IrC}_2\text{B}_9\text{H}_{11}]^+$ . In particular, it reacts with cyclopentadienide anions and arenes giving corresponding derivatives  $3\text{-}(\eta\text{-C}_5\text{H}_4\text{R})\text{-}3,1,2\text{-IrC}_2\text{B}_9\text{H}_{11}$  (**3a,b**) and  $[3\text{-}(\text{arene})\text{-}3,1,2\text{-IrC}_2\text{B}_9\text{H}_{11}]^+$  (**1f,g**) (Scheme 3).

#### X-ray diffraction study

The structures of **1ePF<sub>6</sub>** and **2BF<sub>4</sub>** were investigated using X-ray diffraction (Figs. 1 and 2). In both cases the iridium is shifted



Scheme 1. Synthesis of (arene)iridacarboranes **1a–e**.



Scheme 2. Synthesis of the tris(acetonitrile) complex **2**.

towards carbon atoms of the *nido*-carborane ligand (Ir–C distances are shorter than Ir–B ones). In the durene cation **1e** arene and C<sub>2</sub>B<sub>3</sub> planes are almost parallel (the dihedral angle is equal to 5.2°). The Ir···C<sub>2</sub>B<sub>3</sub> distance in **1e** (1.577 Å) is very close to that in the cyclopentadienyl complexes  $3\text{-}(\eta\text{-C}_5\text{R}_5)\text{-}3,1,2\text{-IrC}_2\text{B}_9\text{H}_{11}$  ( $\text{R} = \text{H}$ , 1.573 Å;  $\text{R} = \text{Me}$ , 1.579 Å) [13]. The Ir···C<sub>6</sub> distance (1.758 Å) is very close to that in the cyclopentadienyl analogs  $[\text{Cp}^*\text{Ir}(\text{arene})]^2+$  (1.744–1.763 Å) [14], but is shorter than the corresponding distances in  $[(\text{diene})\text{Ir}(\text{arene})]^+$  (1.770–1.810 Å) [15], suggesting stronger Ir–arene bonding in the Ir(III) complexes.

Noteworthy, the Ir···C<sub>2</sub>B<sub>3</sub> distance in the acetonitrile cation **2** (1.539 Å) is somewhat shorter than the corresponding distance in **1e** (1.577 Å). Probably, the Ir–Carb bond strengthening is caused by weaker bonding with acetonitrile ligands vs. durene (so called trans influence). Moreover, the shortening of the Ir···C<sub>2</sub>B<sub>3</sub> distance in **2** is accompanied by significant elongation of the cage C–C bond (1.724 Å in **2** vs. 1.664 Å in **1e**).

#### Metal–benzene bonding in $[3\text{-}(\text{arene})\text{-}3,1,2\text{-MC}_2\text{B}_9\text{H}_{11}]^+$ ( $\text{M} = \text{Rh}, \text{Ir}$ )

To compare the M–C<sub>6</sub>H<sub>6</sub> bonding in rhoda- and iridacarboranes with that in the cyclopentadienyl analogs  $[(\text{C}_5\text{R}_5)\text{M}(\text{C}_6\text{H}_6)]^{2+}$  ( $\text{M} = \text{Rh}, \text{Ir}; \text{R} = \text{H}, \text{Me}$ ), we carried out energy decomposition analysis (EDA) [16]. According to the EDA method, the interaction energy between the bonding fragments  $\Delta E_{\text{int}}$  can be divided into three main components:

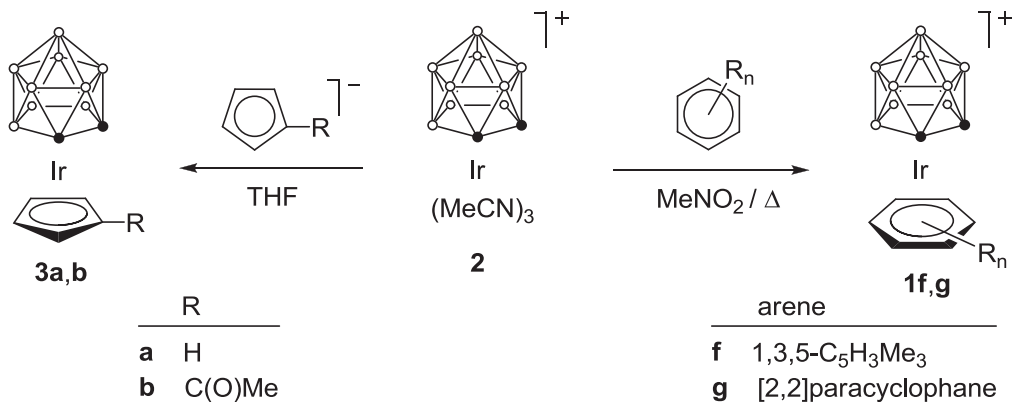
$$\Delta E_{\text{int}} = \Delta E_{\text{elstat}} + \Delta E_{\text{Pauli}} + \Delta E_{\text{orb}}$$

$\Delta E_{\text{elstat}}$  is the electrostatic interaction energy between the fragments with a frozen electron density distribution,  $\Delta E_{\text{Pauli}}$  presents the repulsive four-electron interactions between occupied orbitals (Pauli repulsion), and  $\Delta E_{\text{orb}}$  refers to the stabilizing orbital interactions. The ratio  $\Delta E_{\text{elstat}}/\Delta E_{\text{orb}}$  indicates the electrostatic/covalent character of the bond. The bond dissociation energy

$$D_e = -(\Delta E_{\text{int}} + \Delta E_{\text{prep}}),$$

where  $\Delta E_{\text{prep}}$  (the fragment preparation energy) is the energy that is necessary to promote the fragments from their equilibrium geometry and electronic ground state to the geometry and electronic state that they have in the optimized structure. This method has already proven its usefulness for the analysis of the nature of metal–C<sub>6</sub>H<sub>6</sub> bonding in the chromium [17], rhenium [18], iron [19], ruthenium [20], and cobalt [21] complexes.

The EDA data for complexes  $[(\text{L})\text{M}(\text{C}_6\text{H}_6)]^{n+}$  in terms of interactions between  $[(\text{L})\text{M}]^{n+}$  and C<sub>6</sub>H<sub>6</sub> fragments are given in Table 1. Let us first discuss the bonding in the cyclopentadienyl complexes  $[(\text{C}_5\text{R}_5)\text{M}(\text{C}_6\text{H}_6)]^{2+}$  ( $\text{M} = \text{Rh}, \text{Ir}; \text{R} = \text{H}, \text{Me}$ ). In general, the iridium complexes have much stronger M–C<sub>6</sub>H<sub>6</sub> bond (by 22–23 kcal mol<sup>-1</sup>) than the rhodium analogs. The Cp methylation leads to considerable decrease of the attractive orbital interaction

Scheme 3. Reactions of **2** with Cp-anions and arenes.

( $\Delta E_{\text{orb}}$ ), whereas the sterical contribution ( $\Delta E_{\text{steric}} = \Delta E_{\text{elstat}} + \Delta E_{\text{Pauli}}$ ) remains almost unchanged. As a result, for the methylated complexes  $[\text{Cp}^*\text{M}(\text{C}_6\text{H}_6)]^{2+}$  the  $\text{M}-\text{C}_6\text{H}_6$  bond is weaker by ca. 35 kcal mol<sup>-1</sup> than for the unsubstituted analogs.

Going from cyclopentadienyl complexes to the carborane analogs, the steric interaction increases and, in addition, the orbital interaction decreases explaining loosening of the  $\text{M}-\text{C}_6\text{H}_6$  bond. The  $\Delta E_{\text{int}}$  values correlate well with the dissociation energies ( $D_e$ ) and the  $\text{M}\cdots\text{C}_6\text{H}_6$  distances. Interestingly, in the case of the iridium complex **1a** ( $[\text{M}(\text{L})]^{\text{n}+} = [\text{IrCarb}]^+$ ) the preparation energy ( $\Delta E_{\text{prep}}$ ) is considerably higher (by 10.9 kcal mol<sup>-1</sup>) than that for rhodium analog. This is explained by different optimized geometries of the  $[3,1,2-\text{IrC}_2\text{B}_9\text{H}_{11}]^+$  fragment in the equilibrium ground state (*pseudocloso*) and in complex **1a** (*creso*) (Fig. 3). The *creso*  $\rightleftharpoons$  *pseudocloso* transformations are well known for rhoda- and iridadicarbollides

[13b,22]. Finally, the energy partitioning suggests that the attractive interactions between  $[(\text{L})\text{M}]^{\text{n}+}$  and  $\text{C}_6\text{H}_6$  fragments are ca. 55% covalent and 45% electrostatic for metallacarboranes, being considerably more covalent for the cyclopentadienyl complexes.

Calculations also revealed that the weakest  $\text{M}-\text{C}_6\text{H}_6$  bonds in metallacarboranes  $[(\text{L})\text{M}(\text{C}_6\text{H}_6)]^{2+}$  ( $\text{M} = \text{Rh}, \text{Ir}$ ) (vs  $[(\text{C}_5\text{R}_5)\text{M}(\text{C}_6\text{H}_6)]^{2+}$ ) correlate with the lowest activation energies for the benzene replacement by MeCN or  $\text{H}_2\text{O}$ . Fig. 4 shows the intrinsic reaction coordinates (IRC) for the primary step, at which the iridium cations  $[(\text{L})\text{Ir}(\text{C}_6\text{H}_6)]^{\text{n}+}$  are attacked by the first MeCN molecule. This step has maximal activation energies, since it is accompanied by the hapticity change of benzene ligand,  $\eta^6$  (complex)  $\rightarrow \eta^3$  ( $\text{L} = \text{C}_5\text{R}_5$ ) or  $\eta^4$  ( $\text{L} = \text{C}_2\text{B}_9\text{H}_{11}$ ) (transition state TS, see Fig. 5). Similar IRC profiles for the primary step of benzene replacement by water (Rh and Ir complexes) and acetonitrile (Rh)

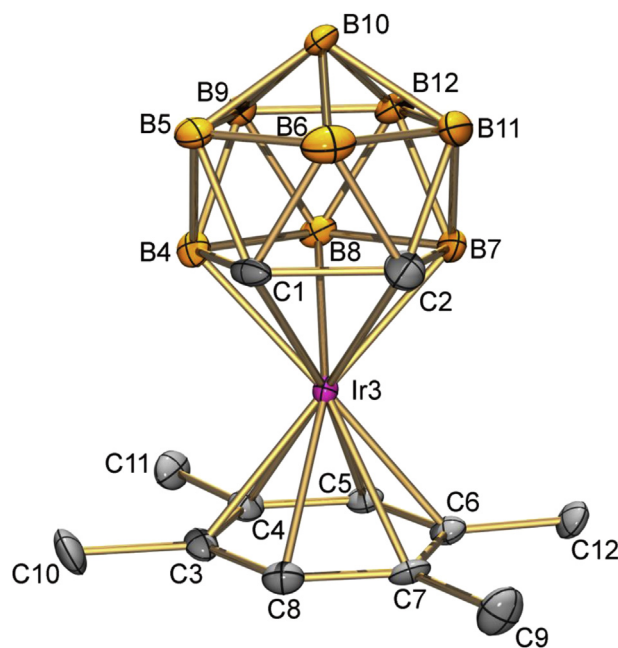


Fig. 1. Structure of cation **1e**. Atoms are represented by 50% thermal ellipsoids. Hydrogen atoms are omitted for clarity. Selected bond lengths [ $\text{\AA}$ ] and angles [ $^\circ$ ]: Ir3–C3 2.271(5), Ir3–C4 2.244(5), Ir3–C5 2.214(5), Ir3–C6 2.271(5), Ir3–C7 2.310(5), Ir3–C8 2.278(5), Ir3–C1 2.157(5), Ir3–C2 2.154(6), Ir3–B4 2.194(6), Ir3–B7 2.192(6), Ir3–B8 2.193(6), C1–C2 1.664(8), C1–B4 1.744(9), C2–B7 1.772(9), B4–B8 1.818(9), B7–B8 1.836(10), C3–C4 1.437(7), C4–C5 1.426(8), C5–C6 1.428(7), C6–C7 1.429(7), C7–C8 1.422(8), C3–C8 1.418(8), C1–C2–B7 111.0(4), C2–B7–B8 104.7(4), B7–B8–B4 107.0(4), B8–B4–C1 105.9(4), B4–C1–C2 111.4(4).

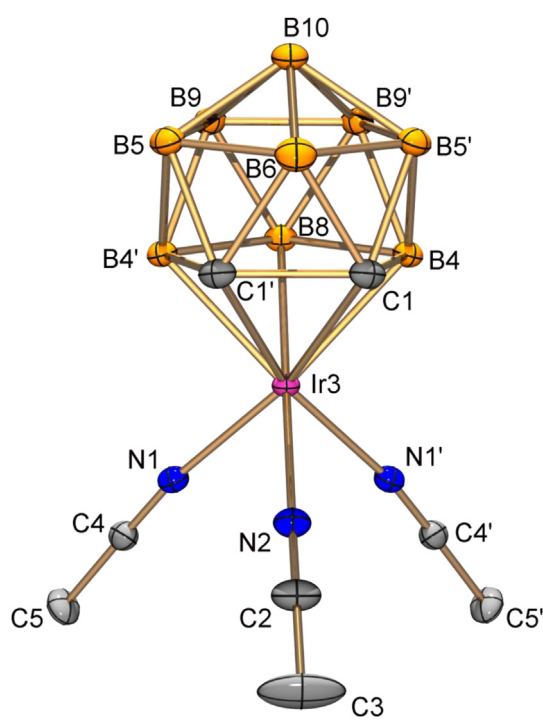


Fig. 2. Structure of cation **2**. Atoms are represented by 50% thermal ellipsoids. Hydrogen atoms are omitted for clarity. Selected bond lengths [ $\text{\AA}$ ] and angles [ $^\circ$ ]: Ir3–C1 2.116(2), Ir3–B4 2.170(2), Ir3–B8 2.206(3), Ir3–N1 2.061(2), Ir3–N2 2.093(2), N1–C4 1.132(2), N2–C2 1.142(3), C1–C14 1.724 ', C1–B4 1.737(3), B4–B8 1.838(3), Ir3–N1–C4 172.3(2), Ir3–N2–C2 173.9(2).

**Table 1**

Results of EDA (energy values in kcal mol<sup>-1</sup>) for the [(L)M(C<sub>6</sub>H<sub>6</sub>)]<sup>n+</sup> (M = Rh, Ir) complexes using C<sub>6</sub>H<sub>6</sub> and the [M(L)]<sup>n+</sup> as Interacting Fragments at BP86/TZ2P.

Fragment [M(L)] <sup>n+</sup>	RhCarb	RhCp	RhCp*	IrCarb	IrCp	IrCp*
ΔE <sub>int</sub>	-71.4	-123.7	-88.4	-92.0	-146.6	-110.8
ΔE <sub>Pauli</sub>	165.8	146.8	146.6	242.5	203.7	212.3
ΔE <sub>elstat</sub> <sup>a</sup>	-107.7 (45.4%)	-98.2 (36.3%)	-97.4 (41.5%)	-155.2 (46.4%)	-134.3 (38.3%)	-138.0 (42.7%)
ΔE <sub>steric</sub>	58.0	48.6	49.2	87.3	69.4	74.3
ΔE <sub>orb</sub> <sup>a</sup>	-129.4 (54.6%)	-172.3 (63.7%)	-137.5 (58.5%)	-179.3 (53.6%)	-216.1 (61.7%)	-185.0 (57.3%)
ΔE <sub>prep</sub>	7.6	4.7	4.6	18.5	6.9	6.5
D <sub>e</sub>	63.8	119.0	83.8	73.5	139.7	104.3
M···C <sub>6</sub> H <sub>6</sub> (centroid)	1.848	1.812	1.846	1.801	1.781	1.803

<sup>a</sup> The values in parentheses give the percentage contribution to the total attractive interactions.

are given in the Supporting Information (Figs. S1–S3). The activation energies (including solvation) are given in Tables 2 and 3. In overall, the barriers for the carborane complexes are ca. 5 kcal mol<sup>-1</sup> lower than for the cyclopentadienyl analogs. Interestingly, the activation energies for the iridium cation **1a** are ca. 4 kcal mol<sup>-1</sup> higher than for the rhodium analog [3-(η-C<sub>6</sub>H<sub>6</sub>)-3,1,2-RhC<sub>2</sub>B<sub>9</sub>H<sub>11</sub>]<sup>+</sup>, correlating well with poorer reactivity of **1a** in benzene replacement.

#### Catalytic activity in oxidative coupling of benzoic acid with alkynes

Taking into account the lability of benzene and acetonitrile ligands, we examined iridacarboranes **1a** and **2** as catalysts for the oxidative coupling of benzoic acid with diphenylacetylene in refluxing *o*-xylene (Scheme 4). This reaction proceeds via C–H activation of *ortho* position of benzoic acid. Silver carbonate was used as a cocatalyst (necessary for the regeneration of the initial catalyst). As can be seen from Table 4, complexes **1a** and **2** catalyze the oxidative coupling to give isocumarin (**3a**) as a sole product in 40–50% yields, in contrast to the reactions catalyzed by rhodacarboranes, which produce mainly naphthalene (**3b**) [8]. The tri(s(acetonitrile)) complex **2** reveals higher catalytic activity than the benzene derivative **1a**, as a consequence of higher lability of acetonitrile ligands. In contrast, using of the SMe<sub>2</sub>-substituted iridadicarbollide chloride [3,3-Cl<sub>2</sub>-4-SMe<sub>2</sub>-3,1,2-IrC<sub>2</sub>B<sub>9</sub>H<sub>10</sub>]<sub>2</sub> [23] or the parent cyclopentadienyl complex [Cp<sup>IrI<sub>2</sub>]<sub>2</sub> in the same reaction results in exclusive formation of naphthalene **3b**. Similar result has been previously obtained using [Cp<sup>\*</sup>IrCl<sub>2</sub>]<sub>2</sub> [4].</sup>

Two pathways of oxidative coupling of benzoic acid with alkynes are well described by the mechanism proposed by Satoh and Miura (Scheme 5) [4]. In particular, the formation of naphthalenes includes the decarboxylation of intermediate **A** giving intermediate

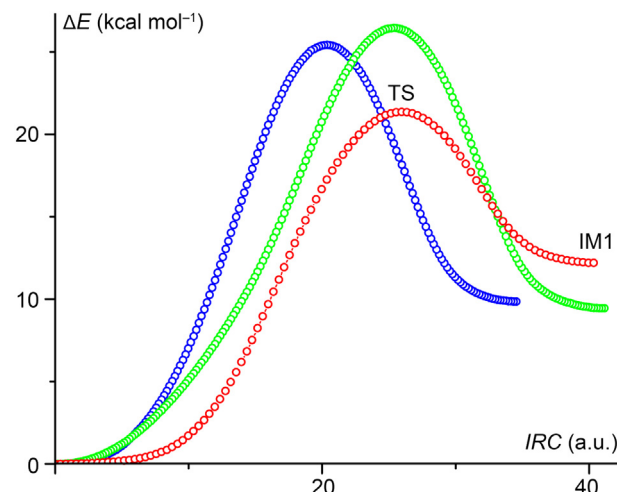


**Fig. 4.** Intrinsic reaction coordinates at PBE/L2 for the primary step of benzene replacement by acetonitrile in the iridium complexes [(L)Ir(C<sub>6</sub>H<sub>6</sub>)]<sup>n+</sup> (L = C<sub>2</sub>B<sub>9</sub>H<sub>11</sub>) (**1a**) red line, L = Cp blue, L = Cp\* green). (For interpretation of the references to color in this figure legend, the reader is referred to the web version of this article.)

**B.** Earlier we shown by DFT-calculations that for (cyclopentadienyl) rhodium complexes the decarboxylation proceeds via two transition states (TS1 and TS2) and have a rather small activation free energies (8–13 kcal mol<sup>-1</sup>), suggesting that the selectivity of oxidative coupling mainly depends from oxidative potential of intermediate **A** [8]. For unsubstituted (cyclopentadienyl)iridium analog the intrinsic reaction coordinates (IRC) have a similar pattern (Fig. 6). In contrast, for Cp<sup>\*</sup>Ir and (C<sub>2</sub>B<sub>9</sub>H<sub>11</sub>)Ir derivatives the

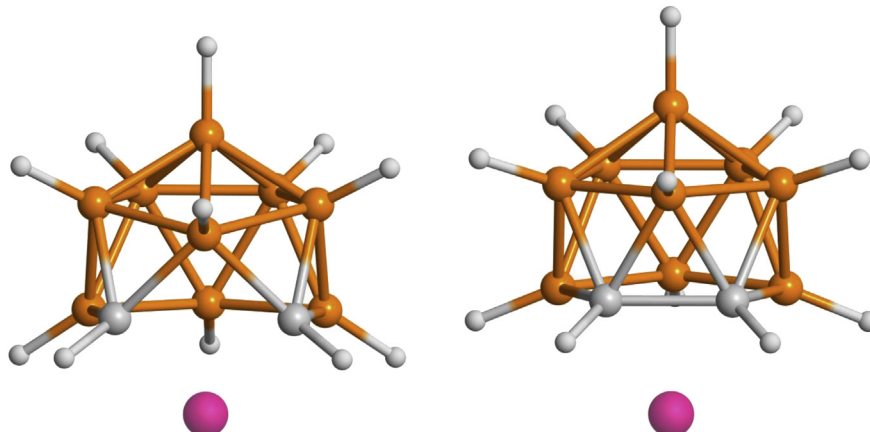


**Fig. 3.** The optimized geometries of the [3,1,2-IrC<sub>2</sub>B<sub>9</sub>H<sub>11</sub>]<sup>+</sup> fragment in the equilibrium ground state (left) and in cation **1a** (right) at BP86/TZ2P.

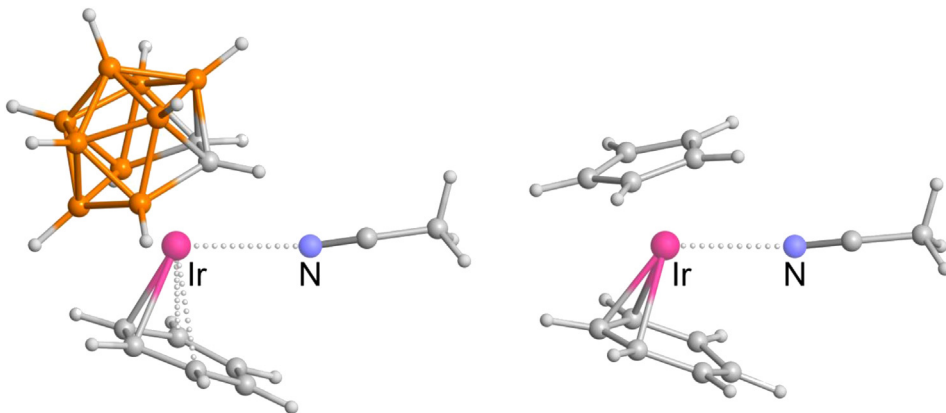


**Fig. 5.** Optimized structures of transition states TS for the attack of **1a** (left) and  $[CpIr(C_6H_6)]^{2+}$  (right) by the first MeCN molecule.

**Table 2**

Activation internal energies  $U_a$ , enthalpies  $H_a$  and free energies  $G_a$  for the primary step of benzene replacement by acetonitrile in the  $[(L)M(C_6H_6)]^{2+}$  complexes (at 298.15 K, in kcal mol<sup>-1</sup>) at BPBE/def2-TZVPP//BPBE/L2.<sup>a</sup>

Complex	$U_a$	$H_a$	$G_a$
$[3-(\eta-C_6H_6)-3,1,2-IrC_2B_9H_{11}]^+$ ( <b>1a</b> )	19.9	19.3	29.7
$[CpIr(C_6H_6)]^{2+}$	24.6	24.0	35.0
$[Cp^*Ir(C_6H_6)]^{2+}$	25.3	24.7	35.6
$[3-(\eta-C_6H_6)-3,1,2-RhC_2B_9H_{11}]^+$	16.3	15.7	25.0
$[CpRh(C_6H_6)]^{2+}$	19.7	19.1	30.4
$[Cp^*Rh(C_6H_6)]^{2+}$	21.4	20.8	28.4

<sup>a</sup> Solvation by acetonitrile is included using the PCM model.

formation of intermediate **B** proceeds via only one transition state TS (Fig. S4 in the Supporting Information). The calculations showed that for the iridium complexes the barriers are only slightly higher (by 0.3–2.9 kcal mol<sup>-1</sup>) than those for the rhodium analogs (Table 5).

For the pentamethylated cyclopentadienyl iridium species the activation energy of decarboxylation is higher by 3.7 kcal mol<sup>-1</sup> and the total energy gain ( $\Delta G_f$ ) is smaller by 1.1 kcal mol<sup>-1</sup> as compared with unsubstituted analog, which can not explain the considerable increasing of the yield of **3b** going from  $[CpIrI_2]_2$  to  $[Cp^*IrCl_2]_2$ . Probably, the donor effect of five Me-groups of the  $Cp^*$  ligand

**Table 3**

Activation internal energies  $U_a$ , enthalpies  $H_a$  and free energies  $G_a$  for the primary step of benzene replacement by water in the  $[(L)M(C_6H_6)]^{2+}$  complexes (at 298.15 K, in kcal mol<sup>-1</sup>) at BPBE/def2-TZVPP//BPBE/L2.<sup>a</sup>

Complex	$U_a$	$H_a$	$G_a$
$[3-(\eta-C_6H_6)-3,1,2-IrC_2B_9H_{11}]^+$ ( <b>1a</b> )	20.5	19.9	28.9
$[CpIr(C_6H_6)]^{2+}$	24.9	24.3	34.6
$[Cp^*Ir(C_6H_6)]^{2+}$	23.9	23.3	33.7
$[3-(\eta-C_6H_6)-3,1,2-RhC_2B_9H_{11}]^+$	15.8	15.2	24.1
$[CpRh(C_6H_6)]^{2+}$	20.2	19.6	28.0
$[Cp^*Rh(C_6H_6)]^{2+}$	19.4	18.8	29.2

<sup>a</sup> Solvation by water is included using the PCM model.

**Table 4**

Catalytic activity of iridacarboranes **1a**, **2** and  $[3,3-Cl_2-4-SMe_2-3,1,2-IrC_2B_9H_{10}]_2$  as well as their cyclopentadienyl analogs in the oxidative coupling of benzoic acid with diphenylacetylene.

Catalyst	Yield, %	
	<b>3a</b>	<b>3b</b>
$[3-(\eta-C_6H_6)-3,1,2-IrC_2B_9H_{11}]^+$ ( <b>1a</b> )	36	—
$[3-(MeCN)_3-3,1,2-IrC_2B_9H_{11}]^+$ ( <b>2</b> )	47	—
$[3,3-Cl_2-4-SMe_2-3,1,2-IrC_2B_9H_{10}]_2$	—	10
$[CpIrI_2]_2$	—	35
$[Cp^*IrCl_2]_2$ <sup>a</sup>	—	79

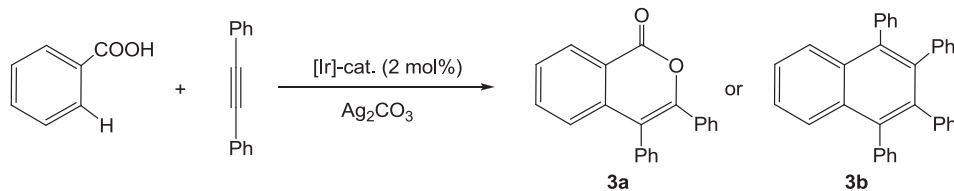
<sup>a</sup> Ref. [4].

reduces the oxidation potential of intermediate **B** facilitating the reductive elimination of the Ir atom with the formation of naphthalene **3b**.

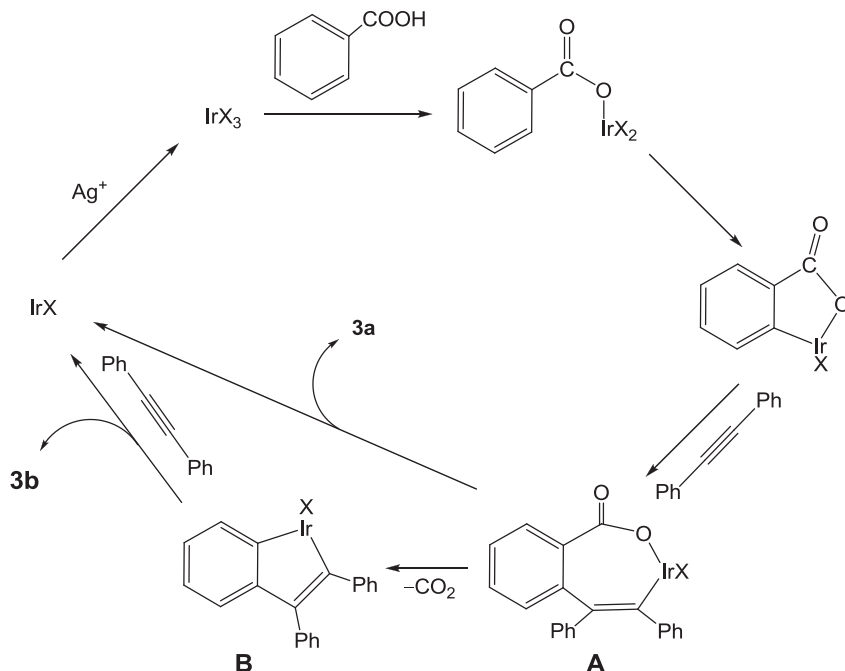
Substitution of the  $Cp$  ligand by dicarbollide-dianion results in the considerable increasing of the decarboxylation barrier up to 18.8 kcal mol<sup>-1</sup>. In addition, the total energy gain for iridacarborane species is smaller by 10.5 kcal mol<sup>-1</sup> than for cyclopentadienyl analog. These data are well correlate with exclusively formation of isocoumarin **3a** in the oxidative coupling reactions using iridacarboranes **1a** and **2**. Nevertheless, we consider that the main reason of this selectivity is caused by the anionic charge of intermediate **A** for the iridacarborane derivatives, which considerably reduces its oxidation potential; this makes the reductive elimination of the Ir atom giving isocoumarin **3a** more favorable than decarboxylation.

## Conclusion

One-pot reaction of  $[(cod)IrCl]_2$  with  $Tl[Tl(\eta-7,8-C_2B_9H_{11})]$  followed by refluxing in trifluoroacetic acid in the presence of arenes was shown to be efficient method for the synthesis of cationic (arene)iridacarboranes **1a–e**. In accordance with stronger Ir–C<sub>6</sub>H<sub>6</sub> bonding than in rhodium analogs, the cation **1a** does not undergo



**Scheme 4.** Oxidative coupling of benzoic acid with diphenylacetylene.



Scheme 5. Plausible mechanism of oxidative coupling.

the arene exchange reaction. Nevertheless, the benzene ligand in **1a** is easily replaced by MeCN giving the tris(acetonitrile) complex **2**. The latter can be used as a synthon of the cationic iridacarborane fragment [3,1,2-IrC<sub>2</sub>B<sub>9</sub>H<sub>11</sub>]<sup>+</sup>, as illustrated by the preparation of its cyclopentadienyl and arene derivatives. Iridacarboranes **1a** and **2** exhibit moderate catalytic activity in the oxidative coupling of benzoic acid with diphenylacetylene in the presence of Ag<sub>2</sub>CO<sub>3</sub> selectively giving 3,4-diphenylisocoumarin. On the other hand, the use of the cyclopentadienyl complexes [(C<sub>5</sub>R<sub>5</sub>)IrCl<sub>2</sub>]<sub>2</sub> as catalysts gives only 1,2,3,4-tetraphenylnaphthalene. DFT-calculations suggest that the selectivity of this reaction is mainly determined by the electronic rather than steric properties of the ligand (C<sub>2</sub>B<sub>9</sub>H<sub>11</sub> or C<sub>5</sub>R<sub>5</sub>) at the iridium atom.

According to the energy decomposition scheme, the Ir–C<sub>6</sub>H<sub>6</sub> bond in benzene complex **1a** is weaker by 20–50 kcal mol<sup>-1</sup> than in cyclopentadienyl analogs [(C<sub>5</sub>R<sub>5</sub>)Ir(C<sub>6</sub>H<sub>6</sub>)]<sup>2+</sup>. It correlates well with

the lowest activation energies for benzene replacement in this cation by acetonitrile or water. The attractive interactions between [3,1,2-IrC<sub>2</sub>B<sub>9</sub>H<sub>11</sub>]<sup>+</sup> and C<sub>6</sub>H<sub>6</sub> fragments are ca. 55% covalent and 45% electrostatic, being considerably more electrostatic than similar interactions with [(C<sub>5</sub>R<sub>5</sub>)Ir]<sup>2+</sup> fragments.

## Experimental

### General

The reactions were carried out under an inert atmosphere in dry solvents, unless otherwise stated. The isolation of products was conducted in air. Starting materials [(cod)IrCl]<sub>2</sub> [24] and Tl[Tl(η-7,8-C<sub>2</sub>B<sub>9</sub>H<sub>11</sub>)] [25] were prepared as described in the literature. <sup>1</sup>H and <sup>11</sup>B{<sup>1</sup>H} NMR spectra ( $\delta$  in ppm) were recorded on a Bruker Avance-400 spectrometer operating at 400.13 and 128.38 MHz, respectively.

### Synthesis of [3-(arene)-3,1,2-IrC<sub>2</sub>B<sub>9</sub>H<sub>11</sub>]PF<sub>6</sub> (1a–cPF<sub>6</sub>)

A mixture of [(cod)IrCl]<sub>2</sub> (100 mg, 0.149 mmol), Tl[Tl(η-7,8-C<sub>2</sub>B<sub>9</sub>H<sub>11</sub>)] (162 mg, 0.30 mmol), and THF (2 ml) was stirred for 1 h. The precipitate of TlCl was centrifuged off and the centrifugate was evaporated *in vacuo*. Arene (1 ml of benzene, toluene or xylene,

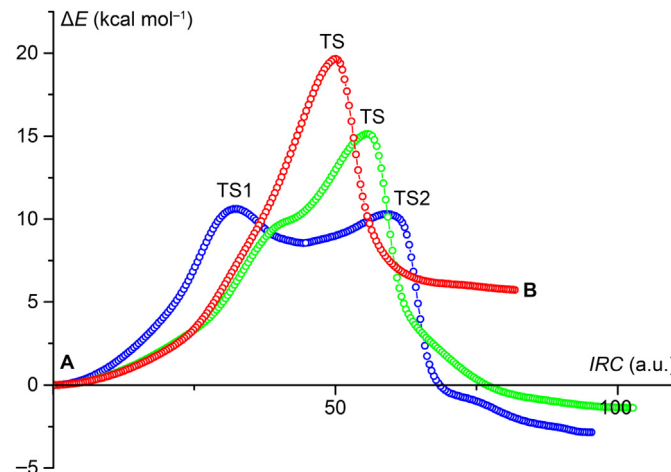


Fig. 6. Intrinsic reaction coordinates at PBE/L2 for the decarboxylation of intermediate **A** (in the case of unsubstituted acetylene) using complexes **1a** (red line), [CpIrCl<sub>2</sub>]<sub>2</sub> (blue) and [Cp\*IrCl<sub>2</sub>]<sub>2</sub> (green). (For interpretation of the references to color in this figure legend, the reader is referred to the web version of this article.)

Table 5

Activation enthalpies ( $H_a$ ) and free energies ( $G_a$ ) as well as total energy gains ( $H_r$  and  $G_r$ ) for the decarboxylation of the intermediate **A** in the presence of rhodium and iridium complexes (in the case of unsubstituted acetylene) at 298.15 K, in kcal mol<sup>-1</sup>.

LM	TS1		TS2		Total energy gain	
	$H_a$	$G_a$	$H_a$	$G_a$	$H_r$	$G_r$
(C <sub>2</sub> B <sub>9</sub> H <sub>11</sub> )Ir	17.92	18.80	—	—	-7.88	3.92
CpIr	9.62	11.04	8.61	10.47	2.36	14.43
Cp*Ir	13.33	14.74	—	—	0.88	13.33
(C <sub>2</sub> B <sub>9</sub> H <sub>11</sub> )Rh	16.79	18.53	—	—	-11.46	-0.24
CpRh	6.56	8.29	6.69	7.76	0.03	11.37
Cp*Rh	5.51	7.50	12.19	13.39	-3.60	7.10

or 300 mg of durene) was added to the residue containing  $\text{Ti}[\text{3-(cod)-3,1,2-IrC}_2\text{B}_9\text{H}_{11}]$ . After cooling to  $-73^\circ\text{C}$ ,  $\text{CF}_3\text{COOH}$  (1.5 ml) and  $(\text{CF}_3\text{CO})_2\text{O}$  (0.5 ml) were added, and the reaction mixture was refluxed with vigorous stirring for 2 h. The solvents were removed *in vacuo* and the residue was extracted with water ( $2 \times 5$  ml). Then an excess of an aqueous  $\text{KPF}_6$  solution was added. The white precipitate that formed was filtered off, washed with water and dried *in vacuo*. The crude product was reprecipitated by ether from acetone solution.

**1aPF<sub>6</sub>**, arene =  $\text{C}_6\text{H}_6$ , yield 27%.  $^1\text{H}$  NMR (acetone- $d_6$ )  $\delta$ : 5.98 (br. s, 2H, CH), 8.04 (s, 6H,  $\text{C}_6\text{H}_6$ ).  $^{11}\text{B}\{^1\text{H}\}$  NMR (acetone- $d_6$ )  $\delta$ : 11.05 (1B), 2.10 (1B), -6.03 (2B), -6.68 (c, 2B), -15.91 (2B), -22.50 (1B). Found (%): C, 17.49; H, 3.00; B, 17.74. Calc. for  $\text{C}_8\text{H}_{17}\text{B}_9\text{F}_6\text{IrP}$  (%): C, 17.54; H, 3.13; B, 17.77.

**1bPF<sub>6</sub>**, arene =  $\text{C}_6\text{H}_5\text{Me}$ , yield 17%.  $^1\text{H}$  NMR (acetone- $d_6$ )  $\delta$ : 2.89 (s, 3H,  $\text{C}_6\text{H}_5\text{Me}$ ), 5.93 (br. s, 2H, CH), 7.92 (m, 5H,  $\text{C}_6\text{H}_5\text{Me}$ ).  $^{11}\text{B}\{^1\text{H}\}$  NMR (acetone- $d_6$ )  $\delta$ : 10.40 (1B), 2.84 (1B), -5.46 (2B), -6.79 (2B), -16.02 (2B), -22.40 (1B). Found (%): C, 19.11; H, 3.37; B, 17.25. Calc. for  $\text{C}_9\text{H}_{19}\text{B}_9\text{F}_6\text{IrP}$  (%): C, 19.24; H, 3.41; B, 17.32.

**1cPF<sub>6</sub>**, arene = 1,2- $\text{C}_6\text{H}_4\text{Me}_2$ , yield 25%.  $^1\text{H}$  NMR (acetone- $d_6$ )  $\delta$ : 2.81 (s, 6H,  $\text{C}_6\text{H}_4\text{Me}_2$ ), 5.85 (br. s, 2H, CH), 7.81 (m, 4H,  $\text{C}_6\text{H}_4\text{Me}_2$ ).  $^{11}\text{B}\{^1\text{H}\}$  NMR (acetone- $d_6$ )  $\delta$ : 9.80 (1B), 4.06 (1B), -4.82 (2B), -6.87 (2B), -16.08 (2B), -22.27 (1B). Found (%): C, 20.61; H, 3.71; B, 16.82. Calc. for  $\text{C}_{10}\text{H}_{21}\text{B}_9\text{F}_6\text{IrP}$  (%): C, 20.86; H, 3.68; B, 16.90.

**1dPF<sub>6</sub>**, arene = 1,3- $\text{C}_6\text{H}_4\text{Me}_2$ , yield 37%.  $^1\text{H}$  NMR (acetone- $d_6$ )  $\delta$ : 2.86 (s, 6H,  $\text{C}_6\text{H}_4\text{Me}_2$ ), 5.81 (br. s, 2H, CH), 7.78 (m, 3H,  $\text{C}_6\text{H}_4\text{Me}_2$ ), 7.84 (s, 1H,  $\text{C}_6\text{H}_4\text{Me}_2$ ).  $^{11}\text{B}\{^1\text{H}\}$  NMR (acetone- $d_6$ )  $\delta$ : 9.80 (1B), 3.54 (1B), -4.92 (2B), -6.82 (2B), -16.06 (2B), -22.23 (1B). Found (%): C, 20.59; H, 3.41; B, 16.48. Calc. for  $\text{C}_{10}\text{H}_{21}\text{B}_9\text{F}_6\text{IrP}$  (%): C, 20.86; H, 3.68; B, 16.90.

**1ePF<sub>6</sub>**, arene = 1,2,4,5- $\text{C}_6\text{H}_2\text{Me}_4$ , yield 23%.  $^1\text{H}$  NMR (acetone- $d_6$ )  $\delta$ : 2.70 (s, 12H,  $\text{C}_6\text{H}_2\text{Me}_4$ ), 5.64 (br. s, 2H, CH), 7.73 (s, 2H,  $\text{C}_6\text{H}_2\text{Me}_4$ ).  $^{11}\text{B}\{^1\text{H}\}$  NMR (acetone- $d_6$ )  $\delta$ : 8.48 (1B), 4.02 (1B), -3.82 (2B), -6.89 (2B), -16.20 (2B), -21.94 (1B). Found (%): C, 23.91; H, 4.14; B, 15.17. Calc. for  $\text{C}_{12}\text{H}_{25}\text{B}_9\text{F}_6\text{IrP}$  (%): C, 23.87; H, 4.17; B, 16.11.

### Synthesis of [3-(MeCN)<sub>3</sub>-3,1,2-IrC<sub>2</sub>B<sub>9</sub>H<sub>11</sub>]PF<sub>6</sub> (2PF<sub>6</sub>)

A solution of **1aPF<sub>6</sub>** (100 mg, 0.18 mmol) in MeCN (2 ml) was refluxed for 1.5 h. The solvent was removed *in vacuo* and the residue was reprecipitated by ether from acetonitrile solution. Yield 95 mg (89%) of **2PF<sub>6</sub>** as a yellow solid.  $^1\text{H}$  NMR (acetonitrile- $d_3$ )  $\delta$ : 1.95 (s, 9H, MeCN), 5.40 (br. s, 2H, CH).  $^{11}\text{B}\{^1\text{H}\}$  NMR (acetonitrile- $d_3$ )  $\delta$ : 16.69 (1B), 6.20 (1B), 0.48 (2B), -4.99 (2B), -6.79 (2B), -22.11 (1B). Found (%): C, 15.95; H, 3.30; N, 6.99; B, 16.42. Calc. for  $\text{C}_8\text{H}_{20}\text{N}_3\text{B}_9\text{F}_6\text{IrP}$  (%): C, 16.21; H, 3.40; N, 7.09; B, 16.41.

### Synthesis of 3-( $\eta$ - $\text{C}_5\text{H}_4\text{R}$ )-3,1,2-IrC<sub>2</sub>B<sub>9</sub>H<sub>11</sub> (**3a,b**)

A mixture of **2PF<sub>6</sub>** (50 mg, 0.084 mmol),  $\text{TiCp}$  (30 mg, 0.112 mmol) or  $\text{Na}[\text{C}_5\text{H}_4\text{C(O)Me}]$  (15 mg, 0.115 mmol), and THF (2 ml) was stirred for 2 h. The solvent was removed *in vacuo* and the residue was filtered through a layer of  $\text{Al}_2\text{O}_3$  (5 cm) in dichloromethane. The solution obtained was concentrated to ca. 0.5 ml and an excess of petroleum ether was added. The white precipitate that formed was filtered off, washed with petroleum ether and dried *in vacuo*.

**3a**, R = H, yield 64%.

**3b**, R =  $\text{C(O)Me}$ , yield 33%.  $^1\text{H}$  NMR (CDCl<sub>3</sub>)  $\delta$ : 2.43 (s, 3H, Me), 4.41 (s, 2H, CH), 5.96 (s, 2H,  $\text{C}_5\text{H}_4$ ), 6.25 (s, 2H,  $\text{C}_5\text{H}_4$ ). Found (%): C, 25.82; H, 4.17; B, 21.60. Calc. for  $\text{C}_9\text{H}_{18}\text{B}_9\text{IrO}$  (%): C, 25.04; H, 4.20; B, 22.54.

### Synthesis of [3-(arene)-3,1,2-IrC<sub>2</sub>B<sub>9</sub>H<sub>11</sub>]PF<sub>6</sub> (1f,g) from 2PF<sub>6</sub>

A mixture of **2PF<sub>6</sub>** (81 mg, 0.137 mmol), mesitylene (1 ml) or [2,2]paracyclophane (116 mg, 0.879 mmol), and nitromethane (1 ml) was refluxed for 1.5 h. The solvent was removed *in vacuo* and the residue was reprecipitated by ether from nitromethane solution to give white solids.

**1fPF<sub>6</sub>**, arene = 1,3,5- $\text{C}_6\text{H}_3\text{Me}_3$ , yield 57%.  $^1\text{H}$  NMR (acetone- $d_6$ )  $\delta$ : 2.83 (s, 9H,  $\text{C}_6\text{H}_3\text{Me}_3$ ), 5.73 (br. s, 2H, CH), 7.78 (m, 3H,  $\text{C}_6\text{H}_3\text{Me}_3$ ).  $^{11}\text{B}\{^1\text{H}\}$  NMR (acetone- $d_6$ )  $\delta$ : 9.21 (1B), 3.93 (1B), -4.96 (2B), -6.92 (2B), -16.07 (2B), -22.14 (1B). Found (%): C, 22.42; H, 3.98; B, 16.51. Calc. for  $\text{C}_{11}\text{H}_{23}\text{B}_9\text{F}_6\text{IrP}$  (%): C, 22.40; H, 3.93; B, 16.50.

**1gPF<sub>6</sub>**, arene = [2,2]paracyclophane, yield 38%.  $^1\text{H}$  NMR (acetone- $d_6$ )  $\delta$ : 3.55 (m, 8H, CH<sub>2</sub>), 5.69 (s, 2H, CH), 7.21 (s, 4H,  $\text{C}_6\text{H}_4$ ), 7.24 (s, 4H,  $\text{C}_6\text{H}_4$ ).  $^{11}\text{B}\{^1\text{H}\}$  NMR (acetone- $d_6$ )  $\delta$ : 10.05 (1B), 1.65 (1B), -6.48 (2B), -7.45 (2B), -16.50 (2B), -23.40 (1B). Found (%): C, 31.63; H, 4.04; B, 14.40. Calc. for  $\text{C}_{18}\text{H}_{27}\text{B}_9\text{F}_6\text{IrP}$  (%): C, 31.89; H, 4.01; B, 14.35.

### Oxidative coupling of benzoic acid with diphenylacetylene (general procedure)

A mixture of benzoic acid (31 mg, 0.25 mmol), diphenylacetylene (89 mg, 0.5 mmol), catalyst (0.005 mmol),  $\text{Cu}(\text{OAc})_2$  (182 mg, 1.00 mmol), and *o*-xylene (2 ml) was refluxed with vigorous stirring for 6 h. The solvent was removed *in vacuo*, and the residue was extracted with diethyl ether. The extract was chromatographed on column with silica gel (1 × 15 cm). Unreacted diphenylacetylene was washed off with petroleum ether. Then the yellow band was collected using diethyl ether as the eluent. After the removal of the solvent *in vacuo*, isocumarin **3a** or naphthalene **3b** was obtained as an yellow oil.

**3a**,  $^1\text{H}$  NMR (CDCl<sub>3</sub>)  $\delta$ : 8.44 (d, 1H,  $J$  = 8.0 Hz); 7.67 (m, 1H); 7.55 (m, 1H); 7.44 (m, 3H), 7.35 (m, 2H), 7.20–7.30 (m, 6H) (cf. [4]).

**3b**,  $^1\text{H}$  NMR (CDCl<sub>3</sub>)  $\delta$ : 6.95–6.97 (m, 10H); 7.32–7.34 (m, 10H); 7.47–7.49 (m, 2H); 7.76–7.78 (m, 2H) (cf. [26]).

### X-ray crystallography

Crystals of **1ePF<sub>6</sub>** were grown up by slow diffusion in two-layer system, petroleum ether and a solution of the complex in acetone. Crystals of **2BF<sub>4</sub>** were obtained by recrystallization from hot nitromethane-anisole mixture (1:1). X-ray diffraction experiments of **1ePF<sub>6</sub>** and **2BF<sub>4</sub>** were carried out with a Bruker Apex 2 diffractometer using graphite monochromated Mo-K $\alpha$  radiation ( $\lambda$  = 0.71073 Å,  $\omega$  - scans) at 100 and 295 K, respectively. The principal crystallographic data, procedures for collecting data, and characteristics of structure refinement are listed in Table 6. The structures were solved by direct methods and refined by the full-matrix least-squares against F<sup>2</sup> in anisotropic approximation for ordered non-hydrogen atoms. H(C) and H(B) atom positions were calculated, and they were refined in isotropic approximation in riding model. Four fluorine atoms of the PF<sub>6</sub><sup>-</sup> anion in **1ePF<sub>6</sub>** are disordered over two sites with site occupancies 0.33: 0.67 and were refined isotropically. The crystal of **1ePF<sub>6</sub>** is twinned. Collected dataset was indexed using Cell\_now software and then intensities of collected reflections were described as superposition of two crystal components with rotation angle equal to 179.7° using HKLF 5 format and BASF instruction. All calculations were performed using the SHELXTL PLUS 5.0 [27] and OLEX2 [28] software.

### Computational details

Geometry optimizations were performed without constraints using the PBE exchange-correlation functional [29], the scalar-

**Table 6**Crystallographic data and structure refinement parameters for **1ePF<sub>6</sub>** and **2BF<sub>4</sub>**.

Compound	<b>1ePF<sub>6</sub></b>	<b>2BF<sub>4</sub></b>
Empirical formula	C <sub>12</sub> H <sub>25</sub> B <sub>9</sub> F <sub>6</sub> IrP	C <sub>8</sub> H <sub>20</sub> B <sub>10</sub> F <sub>4</sub> IrN <sub>3</sub>
Molecular weight	603.78	534.57
Crystal system	Monoclinic	Orthorhombic
Space group	P <sub>2</sub> 1/c	Pnma
<i>a</i> (Å)	10.8651(9)	15.2750(7)
<i>b</i> (Å)	9.6330(8)	10.6572(5)
<i>c</i> (Å)	19.2709(16)	11.1848(5)
$\beta$ (°)	92.1310(10)	90
<i>V</i> (Å <sup>3</sup> )	2015.6(3)	1820.76(14)
<i>Z</i>	4	4
<i>D<sub>calcd</sub></i> (g cm <sup>-3</sup> )	1.990	1.950
<i>T</i> , K	100	295
$\mu$ (cm <sup>-3</sup> )	67.54	73.67
Absorption correction	multi-scan	multi-scan
<i>T<sub>max</sub></i> / <i>T<sub>min</sub></i>	0.4356/0.2754	0.230/0.125
Collected reflections	5309	27,316
Independent reflections	5309	3732 ( <i>R<sub>int</sub></i> = 0.0311)
Observed reflections	4949	3395
( <i>I</i> > 2σ( <i>I</i> ))		
Parameters	263	135
<i>R</i> <sub>f</sub> (on <i>F</i> for observed reflections)	0.0295	0.0185
<i>wR</i> <sub>2</sub> (on <i>F</i> <sup>2</sup> for all reflections)	0.0879	0.0515
Weighting scheme	$w^{-1} = \sigma^2(F_0^2) + (aP)^2 + bP$ , where $P = 1/3(F_0^2 + 2F_c^2)$	
<i>a</i>	0.0580	0.0370
<i>b</i>	8.3585	—
<i>F</i> (000)	1152	1008
Goodness-of-fit	1.005	1.020
Largest diff. peak and hole (e Å <sup>-3</sup> )	1.910 and -2.031	3.113 and -1.398

relativistic Hamiltonian [30], atomic basis sets of generally contracted Gaussian functions [31], and a density-fitting technique [32] as implemented in a recent version of Priroda code [33]. The all-electron triple-ζ basis set L2 (close to cc-pVTZ) [34] augmented by two polarization functions was used.

The bonding interactions were studied by means of Morokuma-Ziegler energy decomposition analysis as implemented in the ADF 2010.02 program package [35]. The calculations were performed using BP86 functional [36,37]. Scalar relativistic effects were considered using the zero-order regular approximation (ZORA) [38]. All-electron ZORA relativistic triple-ζ basis set augmented by two polarization functions TZ2P was used.

The transition state search was performed using PBE and BPBE exchange-correlation functionals [29,36] with Priroda software. The all-electron triple-ζ basis set L2 augmented by two polarization functions was used for all elements. Frequency calculations were performed to confirm the nature of the stationary points to yield one imaginary frequency for the transition states and none for the minima. The path of the reaction was traced from the transition state to the product and back to the reactant using the Intrinsic Reaction Coordinate method (IRC) [39]. The ChemCraft program [40] was used for molecular modeling and visualization.

## Acknowledgments

This work was supported by Russian Foundation for Basic Research (grant # 15-03-04057).

## Appendix A. Supplementary data

Supplementary data related to this article can be found at <http://dx.doi.org/10.1016/j.jorgchem.2015.01.022>.

## References

- [1] K.A. Kushch, V.V. Lavrushko, Yu.S. Misharin, A.P. Moravsky, A.E. Shilov, *New J. Chem.* 7 (1983) 729–733.
- [2] (a) A.E. Shilov, G.B. Shulpin, *Chem. Rev.* 97 (1997) 2879–2932;  
(b) A.E. Shilov, G.B. Shulpin, *Activation and Catalytic Reactions of Saturated Hydrocarbons in the Presence of Metal Complexes*, Kluwer Academic Publishers, Dordrecht/Boston/London, 2000, p. 548.
- [3] (a) T. Satoh, M. Miura, *Chem. Eur. J.* 16 (2010) 11212;  
(b) G. Song, F. Wang, X. Li, *Chem. Soc. Rev.* 41 (2012) 3651–3678;  
(c) F.W. Patureau, J. Wencel-Delord, F. Glorius, *Aldrichim. Acta* 45 (2012) 31–41.
- [4] K. Ueura, T. Satoh, M. Miura, *J. Org. Chem.* 72 (2007) 5362–5367.
- [5] M.F. Hawthorne, D.C. Young, T.D. Andrews, D.V. Howe, R.L. Pilling, A.D. Pitts, M. Reintjes, L.F. Warren, P.A. Wegner, *J. Am. Chem. Soc.* 90 (1968) 879–896.
- [6] (a) J.A. Long, T.B. Marder, P.E. Behnken, M.F. Hawthorne, *J. Am. Chem. Soc.* 106 (1984) 2979–2989;  
(b) A.K. Saxena, N.S. Hosmane, *Chem. Rev.* 93 (1993) 1081–1124;  
(c) A. Felekidis, M. Goblet-Stachow, J.F. Liegeois, B. Pirotte, J. Delarge, A. Demonceau, M. Fontaine, A.F. Noels, I.T. Chizhevsky, T.V. Zinevich, V.I. Bregadze, F.M. Dolgushin, A.I. Yanovsky, Yu.T. Struchkov, *J. Organomet. Chem.* 536–537 (1997) 405–412;  
(d) I.T. Chizhevsky, *Coord. Chem. Rev.* 251 (2007) 1590–1619.
- [7] (a) N.S. Hosmane (Ed.), *Boron Science: New Technologies and Applications*, CRC Press, 2011;  
(b) H. Shen, H.S. Chan, Z. Xie, *Organometallics* 25 (2006) 5515–5517;  
(c) H. Shen, Z. Xie, *Organometallics* 27 (2008) 2685–2687;  
(d) Y.H. Zhu, N.S. Hosmane, *J. Organomet. Chem.* 747 (2013) 25–29.
- [8] D.A. Loginov, A.O. Belova, A.R. Kudinov, *Izv. Akad. Nauk. Ser. Khim.* (2014) 983–986 [*Russ. Chem. Bull.* 63, 2014, 983–986 (Engl. Transl.)].
- [9] D.A. Loginov, A.O. Belova, Z.A. Starikova, P.V. Petrovskii, A.R. Kudinov, *Mend. Commun.* 21 (2011) 4–6.
- [10] I.U. Khand, P.L. Pauson, W.E. Watts, *J. Chem. Soc. C* (1968) 2257–2260.
- [11] D.A. Loginov, M.M. Vinogradov, Z.A. Starikova, P.V. Petrovskii, A.R. Kudinov, *Izv. Akad. Nauk. Ser. Khim.* (2004) 1871–1874 [*Russ. Chem. Bull.* 53, 2004, 1949–1953 (Engl. Transl.)].
- [12] M. Corsini, S. Losi, E. Grigotti, F. Rossi, P. Zanello, A.R. Kudinov, D.A. Loginov, M.M. Vinogradov, Z.A. Starikova, *J. Solid State Electrochem.* 11 (2007) 1643–1653.
- [13] (a) X.L.R. Fontaine, N.N. Greenwood, J.D. Kennedy, K. Nestor, M. Thornton-Pett, S. Hermanek, T. Jelinek, B. Stibr, *J. Chem. Soc. Dalton Trans.* (1990) 681–689;  
(b) D.A. Loginov, Z.A. Starikova, M. Corsini, P. Zanello, A.R. Kudinov, *J. Organomet. Chem.* 747 (2013) 69–75.
- [14] (a) H. Amouri, M. Gruselle, J. Vaissermann, M.J. McGlinchey, G. Jaouen, *J. Organomet. Chem.* 485 (1995) 79–84;  
(b) D.A. Herbeian, C.S. Schmidt, W.S. Sheldrick, C. van Wullen, *Eur. J. Inorg. Chem.* (1998) 1991–1998;  
(c) J. Moussa, L.-M. Chamoreau, K. Boubekeur, H. Amouri, M.N. Rager, D.B. Grotjahn, *Organometallics* 27 (2008) 67–71.
- [15] (a) J. Muller, Ke Qiao, R. Schubert, M. Tschampel, *Z. Naturforsch. B Chem. Sci.* 48 (1993) 1558–1564;  
(b) C. Teijel, M.A. Ciriano, V. Passarelli, J.A. Lopez, B. de Bruin, *Chem. Eur. J.* 14 (2008) 10985–10998.
- [16] For reviews see: (a) G. Frenking, *J. Organomet. Chem.* 635 (2001) 9–23;  
(b) G. Frenking, K. Wichmann, N. Fröhlich, C. Loschen, M. Lein, J. Frunzke, V.M. Rayon, *Coord. Chem. Rev.* 238 (2003) 55–82;  
(c) G. Frenking, A. Krapp, *J. Comput. Chem.* 28 (2007) 15–24;  
(d) T. Ziegler, J. Autschbach, *Chem. Rev.* 105 (2005) 2695–2722.
- [17] S. Erhardt, G. Frenking, *J. Organomet. Chem.* 694 (2009) 1091–1100.
- [18] E.A. Trifonova, D.S. Perekalin, K.A. Lysenko, A.R. Kudinov, *J. Organomet. Chem.* 727 (2013) 60–63.
- [19] (a) A.R. Kudinov, P. Zanello, R.H. Herber, D.A. Loginov, M.M. Vinogradov, A.V. Vologzhanina, Z.A. Starikova, M. Corsini, G. Giorgi, I. Nowik, *Organometallics* 29 (2010) 2260–2271;  
(b) D.A. Loginov, M.M. Vinogradov, Z.A. Starikova, A.R. Kudinov, *Izv. Akad. Nauk. Ser. Khim.* (2013) 1262–1267 [*Russ. Chem. Bull.* 62, 2013, 1262–1267 (Engl. Transl.)].
- [20] D.S. Perekalin, E.A. Trifonova, Y.V. Nelyubina, A.R. Kudinov, *J. Organomet. Chem.* 754 (2014) 1–4.
- [21] (a) D.A. Loginov, A.A. Pronin, L.S. Shul'pina, E.V. Mutseneck, Z.A. Starikova, P.V. Petrovskii, A.R. Kudinov, *Izv. Akad. Nauk. Ser. Khim.* (2008) 535–539 [*Russ. Chem. Bull.* 57, 2008, 546–551 (Engl. Transl.)];  
(b) D.A. Loginov, A.A. Pronin, Z.A. Starikova, A.V. Vologzhanina, P.V. Petrovskii, A.R. Kudinov, *Eur. J. Inorg. Chem.* (2011) 5422–5429.
- [22] M.M. Vinogradov, Z.A. Starikova, D.A. Loginov, A.R. Kudinov, *J. Organomet. Chem.* 738 (2013) 59–65.
- [23] A.R. Kudinov, D.S. Perekalin, P.V. Petrovskii, *Izv. Akad. Nauk. Ser. Khim.* (2001) 1269–1270 [*Russ. Chem. Bull.* 50, 2001, 1334–1335 (Engl. Transl.)].
- [24] R.H. Crabtree, J.M. Quirk, H. Felkin, T. Fillebeen-Khan, *Synth. React. Inorg. Met. Org. Chem.* 12 (1982) 407–413.
- [25] H.D. Smith, M.F. Hawthorne, *Inorg. Chem.* 13 (1974) 2312–2316.
- [26] T. Uto, M. Shimizu, K. Ueura, H. Tsurugi, T. Satoh, M. Miura, *J. Org. Chem.* 73 (2008) 298–300.
- [27] G.M. Sheldrick, *Acta Cryst. A* 64 (2008) 112–122.

- [28] O.V. Dolomanov, L.J. Bourhis, R.J. Gildea, J.A.K. Howard, H. Puschmann, *J. Appl. Cryst.* 42 (2009) 339–341.
- [29] J.P. Perdew, K. Burke, M. Ernzerhof, *Phys. Rev. Lett.* 77 (1996) 3865–3868.
- [30] K.G. Dyall, *J. Chem. Phys.* 100 (1994) 2118–2127.
- [31] D.N. Laikov, *Chem. Phys. Lett.* 416 (2005) 116–120.
- [32] D.N. Laikov, *Chem. Phys. Lett.* 281 (1997) 151–156.
- [33] D.N. Laikov, Yu.A. Ustynyuk, *Izv. Akad. Nauk. Ser. Khim.* (2005) 804–810 [*Russ. Chem. Bull.* **54**, 2005, 820–826 (Engl. Transl.)].
- [34] T.H. Dunning Jr., *J. Chem. Phys.* 90 (1989) 1007–1023.
- [35] G. te Velde, F.M. Bickelhaupt, S.J.A. van Gisbergen, C. Fonseca Guerra, E.J. Baerends, J.G. Snijders, T. Ziegler, *J. Comput. Chem.* 22 (2001) 931–967.
- [36] A.D. Becke, *Phys. Rev. A* 38 (1988) 3098–3100.
- [37] J.P. Perdew, *Phys. Rev. B* 33 (1986) 8822–8824.
- [38] E. van Lenthe, E.J. Baerends, J.G. Snijders, *J. Chem. Phys.* 99 (1993) 4597–4610.
- [39] K. Fukui, *Acc. Chem. Res.* 14 (1981) 363–368.
- [40] G.A. Zhurko, *ChemCraft* 1.6, 2008. <http://www.chemcraftprog.com>.